JOURNAL OF APPLIED ELECTROCHEMISTRY 23 (1993) 66–71

On the kinetics of lead electrodeposition in fluorosilicate electrolyte Part I: Inhibiting effect of sodium lignin sulphonate

L. MURESAN, L. ONICIU

University of Cluj-Napoca, Faculty of Chemistry, 3400 Cluj Napoca, Romania

R. WIART

UPR 15 du CNRS "Physique des liquides et Electrochimie", Université Pierre et Marie Curie, tour 22, 4 place Jussieu, 75252 Paris, Cedex 05, France

Received 1 April 1992; revised 10 June 1992

The kinetics of lead electrodeposition in Betts type electrolytes was investigated by electrode impedance measurements. In the absence of additives, the complex plane impedance plots exhibit two separate capacitive features and a low-frequency inductive loop. The sizes and proper frequencies of the capacitive loops are influenced by the current density, the electrode rotation speed and the presence of sodium lignin sulphonate (LS), a colloidal organic additive used in practice as levelling agent. The low-frequency inductive loop, connected to the active area where lead is deposited, disappears with the LS-containing electrolyte. A reaction model is proposed in which the charge transfer reaction is coupled to the formation of adsorbed complexed species able to inhibit lead deposition before diffusing towards the bulk solution. The inhibiting effect of LS additive is discussed in terms of changes in the kinetic parameters of reactions.

1. Introduction

In previous work the effects of some organic additives, used in lead electrorefining by the Betts process, on the structure and morphology of cathodic deposits were determined [1]. It was shown that sodium lignin sulphonate (LS) and an extract of horse chestnut (HCE), used as levelling agents, have a beneficial effect on the quality of the lead deposits, leading to smooth layers with specific fibre textures [1,2].

In the presence of LS, two kinds of structures can be distinguished. At low current densities, the deposits are poorly crystallized and do not present any specific orientation nor specific morphology. At higher current densities, a complex texture was demonstrated by X-ray diffraction, characterized by dihedral grains with perpendicular (2 1 1) planes.

With the simultaneous presence of LS and HCE, the deposits are better crystallized and a weak [2 1 1] texture was detected on pyramid-shaped grains at low current densities. At high current densities, the deposits still reveal a dihedral morphology, due to the dominating influence of LS.

It has also been shown that these two levelling agents increase the cathodic polarization and this inhibiting effect is particularly sensitive to electrolyte stirring [1]. So a particular interest arises in understanding the influence of these additives on the electrode kinetics.

Few investigations have been devoted to the mechanism of lead electrocrystallization in the presence of additives [2–5] and to our knowledge no detailed reaction mechanism has been developed in fluorosilicate electrolyte.

The aim of the present work is to investigate lead electrocrystallization in fluorosilicate electrolyte by impedance measurements and to propose a reaction path to account for the main experimental features observed in both the absence and presence of sodium lignin–sulphonate, used as levelling agent in the Betts process [6]. The influence of the additive on the kinetic parameters of the elementary steps of the reaction scheme will be discussed. In a subsequent paper, the kinetics for lead electrocrystallization in the presence of horse-chestnut extract, used alone, or in combination with lignin-sulphonate, will be analysed.

2. Experimental procedure

The electrolyte used in all experiments was a solution of 80 g dm^{-3} H_2SiF_6 and 80 g dm^{-3} Pb^{2+} as $PbSiF_6$, prepared from analytical grade purity chemicals dissolved in bi-ionexchanged water. The experiments were carried out with a rotating disc working electrode made of titanium, of surface area 1.13 cm^2. Before electrolysis, the electrode surface was polished with emery paper (grit 1200). The electrode rotation speed was electronically controlled and varied from 100 to 1200 r.p.m.

A large sheet of pure lead was used as counter electrode and the saturated calomel reference electrode (SCE) was protected by a KNO_3 salt bridge. The cell temperature was held at 25 ± 0.5°C.

0021-891X

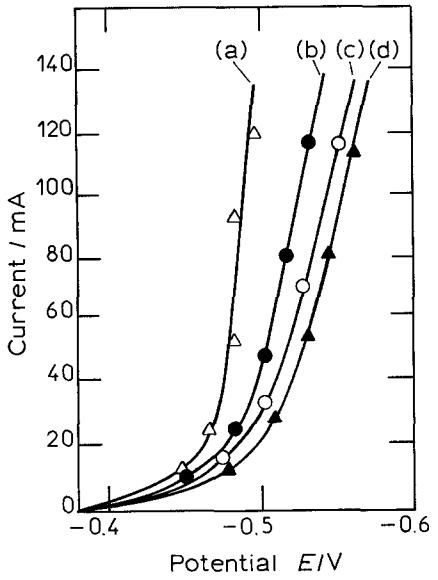

Fig. 1. Polarization curves corrected for ohmic drop (a) in the additive-free electrolyte and (b–d) in the presence of 3 g dm^{-3} LS, at various rotation speeds: (a, b) 1200 r.p.m., (c) 400 r.p.m., (d) 100 r.p.m.

The electrode impedance was measured under potentiostatic conditions using a frequency response analyser between 12 mHz and 60 kHz. The steady-state current–potential curves were plotted from the current and potential values measured during the impedance measurements and they were corrected for ohmic drop.

3. Results

3.1. *Current–potential curves*

In Fig. 1, a set of polarization curves drawn in the absence and in the presence of 3 g dm^{-3} lignin-sulphonate (LS) (a concentration most commonly used in industrial practice), at different rotation speeds, are presented.

It has to be mentioned that without any additive, the development of the surface of the working electrode during lead deposition leads to a lower reproducibility of polarization curves than with the presence of LS, which stabilizes the electrolysis conditions.

The addition of LS shifts the polarization curves towards increasingly negative potentials. At a given potential, the current increases with the rotation speed, thus indicating a stronger inhibition at lower electrolyte stirring.

3.2. *Impedance measurements*

The impedance diagrams recorded over the whole polarization range exhibit two capacitive features and a low frequency inductive loop in the absence of any additive (Fig. 2) and only two capacitive features in the presence of 3 g dm^{-3} LS (Fig. 3).

The mean double layer capacity calculated from the apex of the high frequency capacitive loop varies between 20 and 120 μF cm^{-2} in the absence of additive and is around 40 μF cm^{-2} in the presence of 3 g dm^{-3}

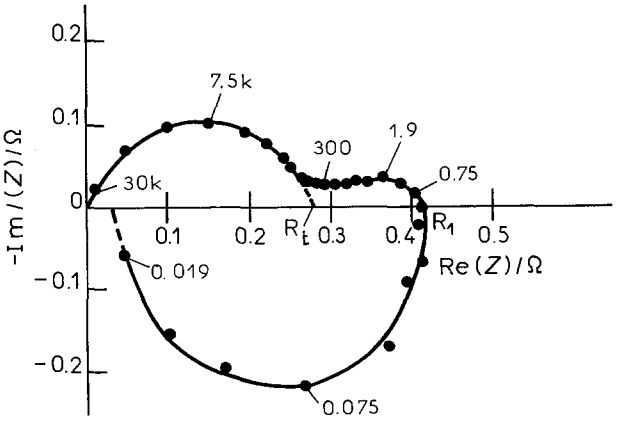

Fig. 2. Complex plane impedance plot recorded in 80 g dm^{-3} H_2SiF_6 and 80 g dm^{-3} Pb; rotation speed 1200 r.p.m.; potential $E = -0.473$ V.

LS. The electrolyte resistance, R_e, was about 1.1 Ω in the absence and 1.5 Ω in the presence of LS, respectively.

The R_tI product of the charge transfer resistance and the current first increases with the electrode polarization and then tends towards an approximately constant value (Fig. 4).

The size of the low-frequency capacitive loop, described by the R_1/R_t ratio, where R_1 is the resistance corresponding to the intermediate frequency at the end of the low-frequency capacitive loop, increases with the electrode polarization (Fig. 5), and decreases with increasing rotation speed (Fig. 6).

The frequency at the apex of the low-frequency capacitive loop, f_1, increases with the electrode rotation speed, as shown in Fig. 7.

The size of the low-frequency inductive loop observed in the absence of LS clearly increases with the electrode polarization at 1200 r.p.m. (Fig. 8). However its variation is not so clear at lower rotation speed, due to a larger propensity to form dendrites.

4. Discussion

Similarly to the case of copper deposition from citrate complexes previously analysed [7], for which the impedance spectra have also revealed a low-frequency capacitive loop dependent on the electrode rotation speed, it will be considered that the discharge of complexed lead ions produces a complex species able to either diffuse away from the electrode or adsorb and inhibit the ion discharge. Consequently the following

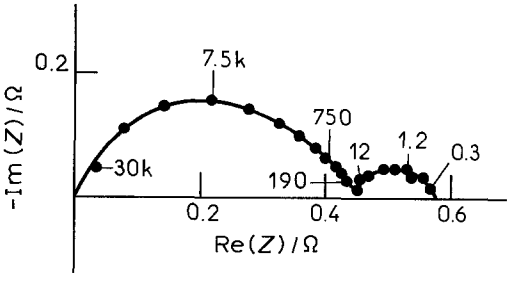

Fig. 3. Complex plane impedance plot recorded in 80 g dm^{-3} H_2SiF_6, 80 g dm^{-3} Pb and 3 g dm^{-3} LS; rotation speed 1200 r.p.m.; potential $E = -0.532$ V.

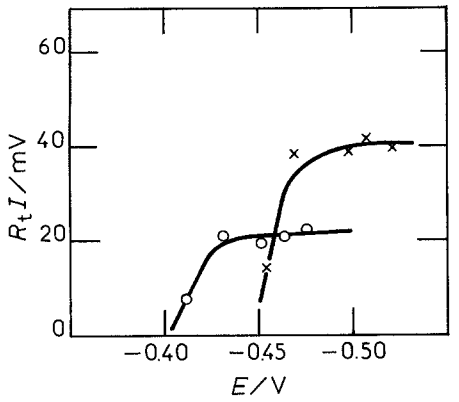

Fig. 4. Potential dependence of the $R_t I$ product (○) for the additive-free electrolyte and (×) with the presence of 3 g dm^{-3} LS; rotation speed 1200 r.p.m.

reaction path will be considered:

$$PbSiF_6 + X + 2e^- \xrightarrow{K_1} Pb + [SiF_6X]^{2-} \quad (I)$$

$$K \downarrow\uparrow K'$$

$$[SiF_6X]^{2-}_{ads} \quad (II)$$

$$\xrightarrow{D} (SiF_6^{2-} + X)_{sol} \quad (II')$$

The charge transfer reaction is assumed to take place from the complexed lead species $PbSiF_6$, which predominates in the solution [8]. The reaction also involves the species X to form a metal atom and a complex $[SiF_6X]^{2-}$ which does not exist in the bulk solution. The complex can either be adsorbed at the interface, thus blocking a fraction θ of the electrode surface area, or diffuse towards the solution with a concomitant decomposition regenerating SiF_6^{2-} and X.

It is difficult to be precise about the nature of the X species. If X denotes H^+, the inhibiting complex might be $[HSiF_6]^-$. In the presence of an inhibitor such as LS, this complex might be $[SiF_6(LS)]^{2-}$, i.e. a colloidal aggregate formed by the adsorption of the anion SiF_6^{2-} on the colloidal particles of LS.

The charge transfer reaction takes place on the unblocked electrode area, $(1 - \theta)$, resulting in a current density i:

$$i = 2FK_1C(1 - \theta) \quad (1)$$

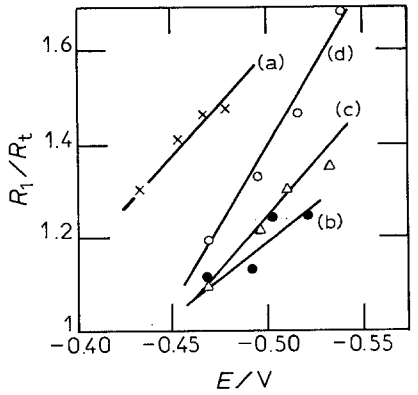

Fig. 5. Potential dependence of the R_1/R_t ratio; (a): additive-free electrolyte, (b–d) with the presence of 3 g dm^{-3} LS. Rotation speed: (a, b) 1200 r.p.m., (c) 400 r.p.m., (d) 100 r.p.m.

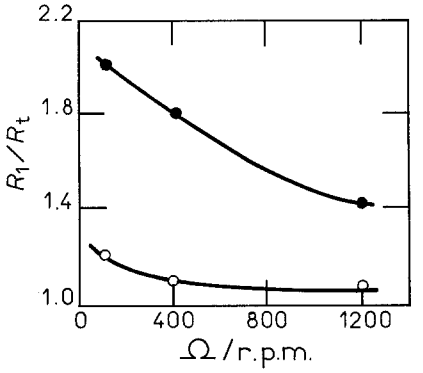

Fig. 6. Rotation speed dependence of the R_1/R_t ratio at potential $E = -0.463$ V; (●) additive-free electrolyte; (○) with the presence of 3 g dm^{-3} LS.

where C is the concentration of $PbSiF_6$ and $K_1 = k_1 \exp(b_1 E)$ as Reaction I is assumed to follow a Tafel activation with cathodic potential E. The parameter k_1 includes both the concentration [X] of the unidentified species X and the rate constant of the reaction. It clearly appears that a rise in the blocking coverage θ with increasing cathodic potential will generate a capacitive impedance.

4.1. *Material balances*

Supposing for simplicity that the adsorbed species $[SiF_6X]^{2-}_{ads}$ does not hinder the adsorption of $[SiF_6X]^{2-}$ ions, but only the charge transfer reaction, the balance for adsorbed species is as follows:

$$\beta \frac{d\theta}{dt} = Kc_0 - K'\theta \quad (2)$$

where c_0 is the concentration of $[SiF_6X]^{2-}$ in the proximity of the electrode and β is the maximal surface concentration of adsorbed species, which can be taken equal to the atom superficial density, $\approx 10^{-9}$ mol cm^{-2}.

For the species $[SiF_6X]^{2-}$ the balance at the interface is:

$$K_1C(1 - \theta) - Kc_0 + K'\theta + D\left(\frac{\partial c}{\partial x}\right)_0 = 0 \quad (3)$$

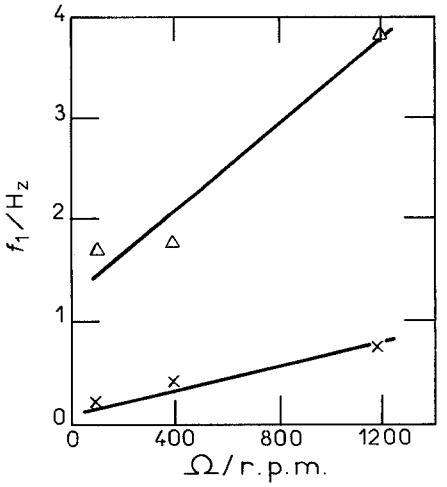

Fig. 7. Rotation speed dependence of the frequency at the apex of the low-frequency capacitive loop, at potential $E = -0.463$ V; (△) additive-free electrolyte, (×) with the presence of 3 g dm^{-3} LS.

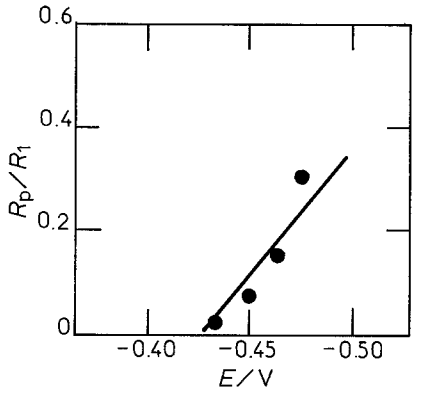

Fig. 8. Potential dependence of the R_p/R_1 ratio in the additive-free electrolyte; rotation speed 1200 r.p.m.

where D is the diffusion coefficient of these species towards the bulk electrolyte.

At a distance x from the electrode, the concentration c of $[SiF_6X]^{2-}$ is given by Fick's second law:

$$\frac{\partial c}{\partial t} = D\frac{\partial^2 c}{\partial x^2} \tag{4}$$

with the boundary conditions for a Nernst diffusion layer of thickness δ:

For $x = \delta$, $c = 0$ (The complex does not exist in the bulk solution.)

For $x = 0$, $c = c_0$

The alternative situation in which the diffusing and inhibiting species were simply SiF_6^{2-} ions has also been considered in the present discussion of results. A similar model was elaborated, but taking into account the concentration c_s of SiF_6^{2-} in the bulk electrolyte ($c_s = 3.8 \times 10^{-4}$ mol cm^{-3}). Then experimental data led to an unacceptable decrease of θ with increasing potential. This result indirectly proves that the discharge of lead cannot be inhibited by adsorbed SiF_6^{2-} species.

4.2. *Steady-state behaviour*

The value of $[SiF_6X]^{2-}_{ads}$ coverage, θ, can be calculated from the steady-state solution of Equations 1–4.

$$\theta = \frac{K}{K'}\frac{i}{2Fk} \tag{5}$$

where $k = D/\delta$.

At a constant rotation speed Ω, for which the thickness δ of the Nernst layer is constant, θ is proportional to the current density. At a constant current density, θ is inversely proportional to $\Omega^{1/2}$.

4.3. *Impedance*

The faradaic impedance $Z_F = \Delta E/\Delta i$ can be calculated by linearizing Equation 1:

$$\frac{1}{Z_F} = \left(\frac{\partial i}{\partial E}\right)_\theta + \left(\frac{\partial i}{\partial \theta}\right)_E \frac{\Delta\theta}{\Delta E} \tag{6}$$

where $(\partial i/\partial E)_\theta$ corresponds to the inverse of the charge transfer resistance R_t such as $R_t i = 1/b_1$. The term $\Delta\theta/\Delta E$ can be obtained by linearizing Equation 2 and 3 and integrating Equation 4 for $x = 0$. So it becomes:

$$\frac{\Delta\theta}{\Delta E} = \frac{\theta\phi}{iZ_F[1 + j\omega\tau'(1 + K\phi/k)]} \tag{7}$$

where ϕ denotes the function $\phi = \tanh(j\omega\tau_d)^{1/2}/(j\omega\tau_d)^{1/2}$, $\tau_d = \delta^2/D$ is the diffusion time constant and $\tau' = \beta/K'$ is the desorption time constant.

Equation 1 gives the final expression for the faradaic impedance, Z_F:

$$Z_F = R_t\left\{1 + \frac{\theta\phi}{(1 - \theta)[1 + j\omega\tau'(1 + K\phi/k)]}\right\} \tag{8}$$

Two limiting cases can be considered according to the relative magnitude of the time constants τ_d and τ'.

(i) A fast diffusion relatively to the adsorption–desorption equilibrium means $\tau_d \ll \tau'$ and $k \ll K$. Then:

$$Z_F = R_t\left[1 + \frac{\theta}{(1 - \theta)(1 + j\omega\tau')}\right] \tag{9}$$

and the low-frequency capacitive loop will be a semicircle.

(ii) A slow diffusion relatively to the adsorption–desorption equilibrium ($\tau' \ll \tau_d$) yields:

$$Z_F = R_t\left(1 + \frac{\theta\phi}{1 - \theta}\right) \tag{10}$$

corresponding to a classical diffusion impedance in series with the charge transfer resistance, with a proportionality of the frequency f_1 at the apex of the diffusion loop to the electrode rotation speed Ω:

$$f_1 = \frac{2.5}{2\pi\tau_d} = \frac{2.5D}{2\pi\delta^2} \approx \Omega \tag{11}$$

Such a proportionality approximately corresponds to the experimental situation observed with the LS-containing electrolyte (Fig. 7).

In both cases, the zero-frequency limit R_1 of Z_F gives the coverage θ:

$$\theta = 1 - \frac{R_t}{R_1} \tag{12}$$

This coverage was estimated from Equation 12 and experimental impedance plots. With the presence of LS in the electrolyte, Figs 9 and 10 show that the experimental data agree with the theoretical predictions of Equation 5: θ is proportional to the current density i and inversely proportional to $\Omega^{1/2}$. The decrease of θ with increasing rotation speed expresses the ejection of inhibiting species $[SiF_6X]^{2-}$ from the electrode surface. In Figs 9 and 10, the curves relative to the additive-free electrolyte do not intersect the origin of axes, at variance with Equation 5. This situation suggests that an important inhibition of lead deposition already preexists in the absence of current

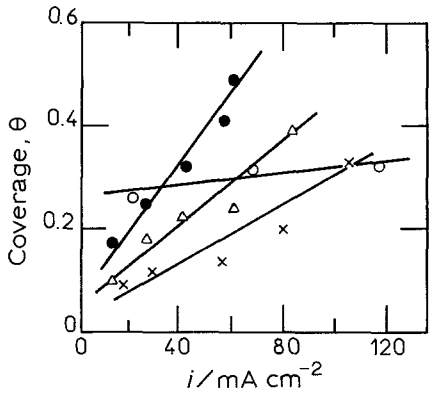

Fig. 9. Electrode coverage by inhibiting species as a function of current density. Electrolyte containing 3 g dm^{-3} LS at various rotation speeds: (•) 100 r.p.m.; (△) 400 r.p.m.; (×) 1200 r.p.m. Additive-free electrolyte: (○) 1200 r.p.m.

and the coverage θ is little modified by the adsorbate produced by Reaction II.

Impedance spectra, simulated from Equation 8 and considering the double layer C_d in parallel with Z_F, confirm that the situation (ii) of a slow diffusion in comparison with the adsorption–desorption equilibrium accounts for the experimental data, especially for LS-containing electrolytes, as illustrated in Fig. 11. This figure reproduces the impedance plot measured at $i = 26\,\text{mA cm}^{-2}$ and a rotation speed $\Omega = 100$ r.p.m. for which δ is equivalent to 5×10^{-3} cm in water when $D = 10^{-5}\,\text{cm}^2\,\text{s}^{-1}$. The parameters used for this figure correspond to a ratio $\tau_d/\tau' = 100$ and $K/k = 0.74$, which characterize a fast desorption process as compared to diffusion.

The values of $R_i i$ corresponding to the plateaux apparent on Fig. 4 give the activation parameter b_1 of K_1 with potential: $b_1 = 40 \pm 2\,\text{V}^{-1}$ for the additive-free electrolyte and $b_1 = 25 \pm 2\,\text{V}^{-1}$ for the LS-containing electrolyte. The lower value is consistent with an inhibiting influence of the LS additive directly at the stage of the charge transfer reaction.

The low-frequency inductive feature, which appears with the additive-free electrolyte, expresses a slow electrode activation with increasing cathodic polarization. It can be ascribed to a slow variation of the

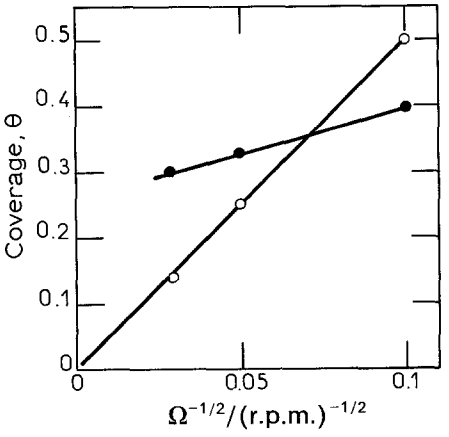

Fig. 10. Electrode coverage by inhibiting species as a function of $\Omega^{1/2}$; (•) additive-free electrolyte; (○) with the presence of 3 g dm^{-3} LS. Current density $i = 56\,\text{mA cm}^{-2}$.

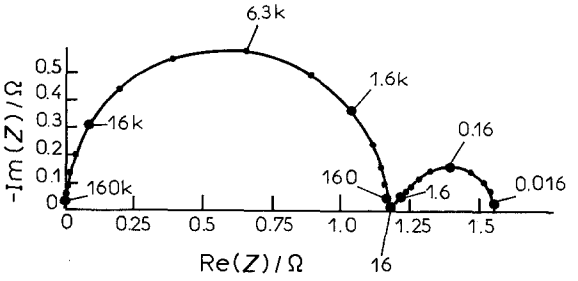

Fig. 11. Complex plane impedance plot simulated by taking $R_i = 1.17\,\Omega$, $i = 26\,\text{mA cm}^{-2}$, $\tau' = 2.5$ ms, $\theta = 0.25$, $C_d = 3 \times 10^{-5}$ F, $\delta = 5 \times 10^{-3}$ cm, $D = 10^{-5}\,\text{cm}^2\,\text{s}^{-1}$.

number of active sites Pb*, as a result of a nucleation process producing active sites and a poisoning process consuming them. These slow processes can be written as:

$$\text{PbSiF}_6 + 2\text{e}^- \xrightarrow{K_3} \text{Pb}^* + \text{SiF}_6^{2-} \qquad \text{(III)}$$

$$\text{Pb}^* \xrightarrow{K_4} \text{Pb} \qquad \text{(IV)}$$

Reaction III is similar to Reaction I, but much slower, and it produces active sites on a fraction θ_1 of the electrode surface, so that Reaction I takes place on the fraction $(1 - \theta)$ of the active sites and the current density i becomes:

$$i = 2FK_1C\theta_1(1 - \theta) \qquad (13)$$

The balance of active sites will be:

$$\beta \frac{d\theta_1}{dt} = K_3(1 - \theta_1) - K_4\theta_1 \qquad (14)$$

whose steady-state solution is:

$$\theta_1 = \frac{K_3}{K_3 + K_4} \qquad (15)$$

An increase of K_3 with E will produce an electrode activation consequent on increasing θ_1. Linearizing Equation 14 gives the equation which governs the relaxation of θ_1:

$$\frac{\Delta\theta_1}{\Delta E} = \frac{(1 - \theta_1)(\delta K_3/\partial E)}{(K_3 + K_4)(1 + j\omega\tau_1)} \qquad (16)$$

where the time constant $\tau_1 = \beta/(K_3 + K_4)$.

In the domain of very low frequencies, this relaxation can generate an additional relaxation process in impedance spectra, corresponding to an inductive loop, and governed by the following equations:

$$\frac{1}{Z_F} = \frac{1}{R_i} + \frac{\partial i}{\partial\theta_1}\frac{\Delta\theta_1}{\Delta E} \qquad (17)$$

$$\frac{1}{Z_F} = \frac{1}{R_i} + \frac{i(1 - \theta_1)}{K_3}\frac{(\partial K_3/\partial E)}{(1 + j\omega\tau_1)} \qquad (18)$$

It must be noted that only a qualitative agreement can be obtained between the equations and the experimental results obtained with the additive-free electrolyte, because of the continuous dendritic growth of lead deposits during electrolysis. In addition, it appears that the LS additive prevents the number of active sites from increasing with increasing

potential, and controls the nucleation rate, thus making the inductive loop disappear.

5. Conclusions

The proposed reaction path for lead electrodeposition from Betts type electrolytes implies a direct discharge of $PbSiF_6$ species coupled to the formation of the complex species $(SiF_6X)^{2-}$ existing only in the proximity of the electrode, where X possibly denotes a proton or a lignin–sulphonate (LS) molecule.

These complex species can be adsorbed on the electrode surface, thus blocking a fraction θ of the area and inhibiting the charge transfer reaction, or it can diffuse towards the electrolyte. In the case where the diffusion process is slow in comparison with the adsorption–desorption equilibrium, such a model explains the main features observed on polarization curves and impedance spectra, especially with the presence of LS used as a levelling agent. A rise in the coverage θ with increasing potential generates a faradaic capacitive impedance characterized by the diffusion time constant. With the presence of LS, this inhibition process by complex adsorbate entirely controls the rate of lead electrodeposition.

The inhibiting influence of the LS additive is interpreted in terms of changes in the kinetic parameters. The adsorption of LS molecules decreases both the double layer capacity and the activation coefficient, b_1, of charge transfer with cathodic potential. It also stabilized the number of active sites for lead deposition, whose potential activation is connected with the inductive feature observed in the additive-free electrolyte.

References

[1] L. Muresan, L. Oniciu, M. Froment and G. Maurin, *Electrochim. Acta* **37** (1992) 2249.
[2] L. Ghergari, L. Oniciu, L. Muresan, A. Pautea, V. A. Topan and D. Ghertoiu, *J. Electroanal. Chem.* **313** (1991) 303–11.
[3] C. J. Krauss, *J. Metals* **28** (11) (1976) 4.
[4] R. C. Kerby and H. E. Jackson, *Can. Metall Q* **17** (1978) 125.
[5] W. Lorenz, *Z. Phys. Chem. Neue Folge* **19** (1959) 377.
[6] A. G. Betts, 'Lead Refining by Electrolysis,' Wiley & Sons, New York (1908).
[7] E. Chassaing, K. Vu Quang and R. Wiart, *J. Appl. Electrochem.* **16** (1986) 591.
[8] Kirk–Othmer, 'Encyclopedia of Chemical Technology', Vol. 12, Interscience Publishers, Wiley & Sons, New York (1967) p. 236.